Lasers in Manufacturing Conference 2019

Challenges and Opportunities for Laser-based Additive Manufacturing of Strain Sensors

Matthias Rehberger[a*], Christian Vedder[a], Johannes Henrich Schleifenbaum[a,b]

[a]*Fraunhofer Institute for Laser Technology ILT, Steinbachstr. 15, 52074 Aachen, German*
[b]*Chair for Digital Additive Production (DAP), RWTH Aachen University, Steinbachstr. 15, 52074 Aachen, Germany*

Abstract

The use of printing and laser technology for additive manufacturing allows for rapid creation of individual sensor structures. Digital production technologies may substitute cost-intensive manual application processes of strain gauges. The development of additive production of individualized, component-connected sensors is shown. Necessary layers and structures of different materials are printed directly onto the component and then laser-treated (sintered, melted, hardened, etc.). In the case of strain gauges the insulation layer, the measuring grid and the encapsulation are applied. In contrast to conventional thermal processes, no complete heating of the component (furnace) or irradiation of the entire surface (flash lamps) is necessary. The energy deposition can be controlled in terms of time and location. This makes the selective coating of temperature-sensitive components possible. A new process chain for an automated way of sensor creation and application offers the widespread use of strain sensors in a new generation of smart products.

Keywords: Laser sintering; strain sensors; Additive manufacturing; Surface Functionalization

1. Motivation

In the last decade, the era of data was proclaimed covered by introducing cyber-physical systems as key enabler for a new generation of interconnected production systems, smart products and digital business models [1]. Data related to mechanical properties such as force, strain or torque can be determined using strain gauges. These sensors, containing a resistive measuring grid on a polymer carrier, are typically manufactured using photolithographic processes for mass fabrication [2]. The application onto a component is a

* Corresponding author. Tel.: +49-241-8906-8300; fax: +49-241-890-6121.
E-mail address: matthias.rehberger@ilt.fraunhofer.de.

manual, time-consuming multi-step gluing process that accounts for the main cost and errors when installing a strain gauge [2].

Additive manufacturing methods allow to overcome limitations of conventionally produced strain gauges. One distinguishes between the additive creation of foil-based strain gauges [3–7] and directly component-connected sensors [8,9]. Foil-based strain gauges usually are printed on polyimide foil as substrates [3–6]. The resistive measuring grid is deposited via Aerosol Jet® [5,6] or inkjet printing [3,4]. Silver [3,4] or Cu-Ni/CuNiMn [5,6] are used as nano-particular ink formulated raw material. Thermal treatment was performed in an oven [3], using flash lamps [6] or laser sintering [4–6]. Due to the use of digital printing technologies a mask free production of individually shaped measuring grid geometries is possible down to lot size 1. The gluing process when applying the strain gauge to a solid component is expected to be comparable to conventional strain gauges. In addition to gained flexibility by using digital printing technologies, the additive manufacturing of component-connected sensors allows to skip subsequent gluing steps, aiming for a fully automatable creation of strain gauges on the target component. Maiwald et al. demonstrate the passivation of an aluminium bar, the printing of a silver strain gauge grid and the encapsulation, all three layers are Aerosol Jet® printed. The thermal treatment is done in an oven process at 350 °C [8]. Another approach is the screen printing of thick film insulation, conducting and resistive layers and the downstream laser post-treatment of the printed layers. Disadvantages are the need for masks (screen printing) and the limitation to 2D or and smooth 3D surfaces [9].

2. Process and Experimental Setup

The experimental part is split into two parts. The first one shows an exemplary selection of laser sintering experiments. The second part presents a process chain for laser-based additive manufacturing of strain sensors. The used ink is a nano-particular silver ink from Advanced Nano Products (DGP 40LT-15C). A Meyerburger PiXDRO LP50 inkjet printer is used, equipped with a Fujifilm Dimatix Spectra SE-128 AA print head of 30 pl nominal droplet volume. The laser system used is an IPG Ytterbium fiber laser with a maximum output power of 200 W (cw, λ = 1070 nm).

2.1. Laser sintering

Conductor tracks made of silver are printed onto microscope slides according to the test pattern shown in Figure 1 (11 tracks per slide, 10 for electrical and one for optical characterization). After printing the samples are dried at 60 °C for 20 min. Each sample is laser treated with different process parameters. The collimated laser beam is deflected by a pair of galvanometer-driven scanning mirrors and focused by an f-theta objective. As a benchmark for oven sintering one sample is sintered thermally at 150 °C for 30 min.

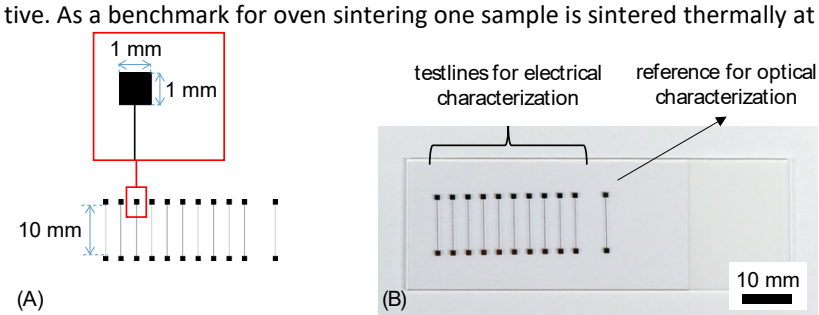

Fig. 1. (A) Test pattern bitmap file for laser sintering tests. (B) Photograph of printed test pattern on microscope slide.

2.2. Laser-based additive manufacturing of strain sensors

The process presented is chosen to combine all advantages of printing component-connected (embedded) sensors and the use of scalable and cost-oriented production technologies. To illustrate the process capabilities, a metallic component of 2 mm stainless steel is chosen to be equipped with an additively manufactured strain gauge using print and laser technologies. The process steps are summarized in Figure 2.

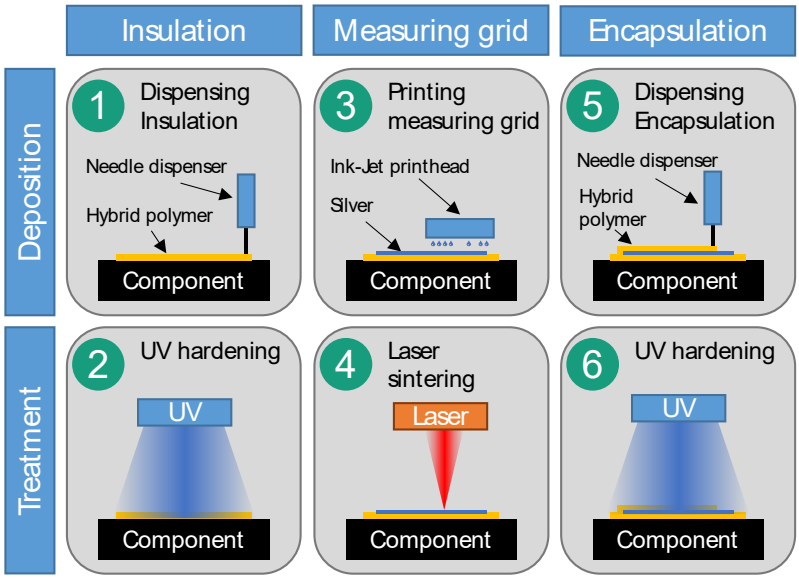

Fig. 2. Process chart for laser-based additive manufacturing of embedded strain sensors

Steps 1+2: For electrical insulation, a passivation layer of hybrid polymer is applied using a needle dispenser. These industrial dispensers are approved for long-term operation and robust material deposition for a wide range of viscosities at low prices. Inorganic-organic hybrid polymers offer robust mechanical properties in addition to UV curing abilities and the possibility to add solvents. This way the material can be inkjet printable for thin film deposition as an option.
Step 3: Inkjet is the printing technology chosen to deposit the metallic measuring grid. Inkjet printing is approved and productively used in industry for product print, décor and textile printing, graphics, packaging, coding and marking, direct-to-shape, ceramic printing, 3D printing, advanced manufacturing or bioprinting [10]. Printing speeds are significantly higher than the smaller feature size achieving Aerosol Jet® technology due to the use of multi nozzle systems (up to thousands of nozzles per printhead) at low investment cost compared to Aerosol Jet®. In addition to that, the quality of Aerosol Jet® printed structures suffers from its spray-like nature and the appearance of overspray [11]. Inkjet printing quality and printable feature sizes improved within the last years due to reduced droplet sizes. While droplets of 1 pl volume are widespread state-of-the-art, the development of print heads for sub-femto liter droplet volumes [12] turned into commercially available systems to print feature sizes down to 1 µm [13]. Thus, inkjet printing is identified to be the promising candidate in terms of cost, productivity and industrial robustness for 2D and smooth 3D surfaces.
Step 4: Sintering of the printed measuring grid is performed using a laser. In contrast to conventional thermal processes, no complete heating of the component (furnace) or irradiation of the entire surface (flash lamps) is necessary. Laser sintering is a purely digital process and the energy deposition can be controlled in

terms of time and location. With its excellent inline capability laser sintering fits to the concept of an automated, scalable and cost-oriented component-connected production of individual sensor geometries. Lasers are also a precise tools for trimming thin film resistors [14], a technology that is further developed to fully automated laser trimming stations used by commercial strain gauge manufacturers like Vishay Precision Group, Inc. [15].

Steps 5+6: For encapsulation the steps 1+2 are repeated with a reduced field size to keep conductors accessible for external connection.

3. Results

3.1. Laser sintering

Optical properties of the UV-cured hybrid polymer and a printed dry silver layer are measured via UV/VIS/NIR spectrometry (see Figure 8 and Figure 9). The absorbance of the silver ink is calculated to A = 1 – R – T to about 50 % at a wavelength of 1070 nm. A process parameter variation is carried out to find the most suitable combination of laser parameters for sintering. Two investigations are shown exemplarily: One focusses on the increase of laser beam intensity I from 1.33 kW/cm² up to 7.02 kW/cm² at fixed processing speeds (areal rate) of F = 0.5 cm²/s resulting in increased fluencies (Figure 3 left). While the oven processed benchmark sample shows resistivities of 82.6 ± 3.5 Ω the resistivities of the laser treated testing structures decrease from 120.2 ± 7.4 Ω (at I = 1.33 kW/cm²) down to 37 ± 0.3 Ω (at I = 7.02 kW/cm²). The other investigation focusses on the increase of processing speed from 0.5 cm²/s up to 2 cm²/s while maintaining the used laser beam intensity at fixed I = 5.63 kW/cm² (Figure 3 right). While increasing the processing speed by a factor of 4 the resistivities of the testing structures only increase by a factor of 1.35, from 38.1 ± 0.7 Ω to 51.6 ± 1.1 Ω.

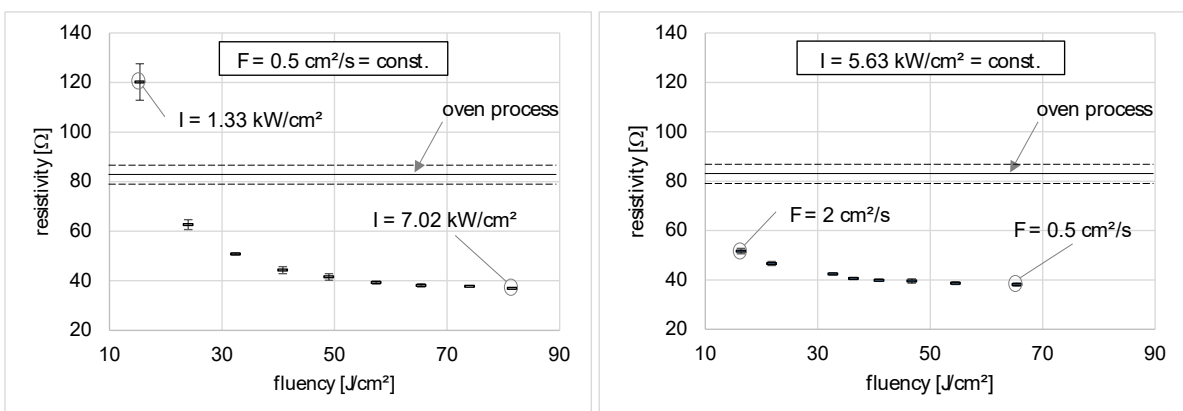

Fig. 3. (left) Resistivity in dependence of fluency while increasing laser beam intensity I, (right) Resistivity in dependence of fluency while increasing processing speed (areal rate F)

Using white-light interferometry (Zygo NetView 7300) the surface roughness, thickness as well as the length and width of the printed and dried as well as oven treated and laser treated structures are measured, which do not differ in a significant way for the described sintering methods and parameters. An exemplary measurement of a laser sintered sample is shown in Figure 4. The layer thickness of the depicted contact pad and the nearby conducting line on the other hand show differences: While the thickness of the contact pad levels up to more than 800 nm, the height of the adjacent conducting track is below 200 nm. This inhomogene-

ous material distribution could be triggered by evaporation-driven material transportation in wet-chemically applied layers comparable to the already known coffee stain effect [16].

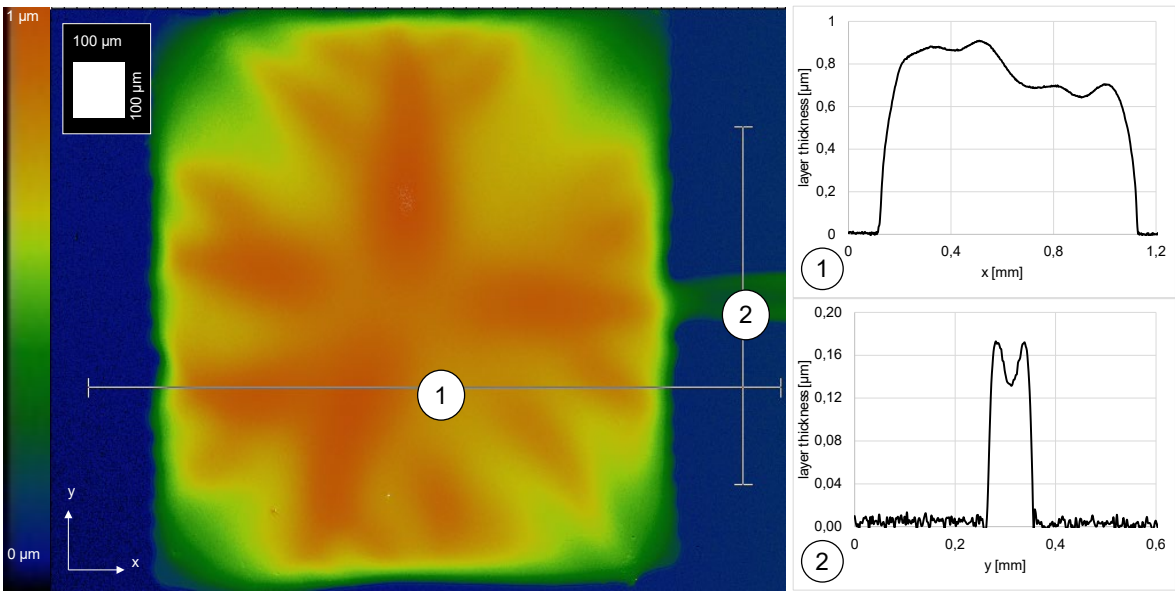

Fig. 4. White-light interferometry picture and layer thickness as well as width measurements of a contact pad (1) and conducting track (2) according to the test pattern in Figure 1

3.2. Laser-based additive manufacturing of strain sensors

Figure 5 shows a photograph of a stainless steel (1.4301) component (120 mm length (100 mm in between the fixation points), 20 mm width at the middle and 2 mm thickness) equipped with a conventionally glued strain gauge (left) and an additively manufactured strain gauge using print and laser technologies according to the process chain described in chapter 2.2. A force is applied to the testing bar in bending load cycles to test for sensor responses under mechanical deformation. The sensor structure is a T-rosette half bridge with two sensitive grids of approx. 4 x 4 mm². The resistances of the grids are 221.4 Ω and 217.3 Ω respectively.

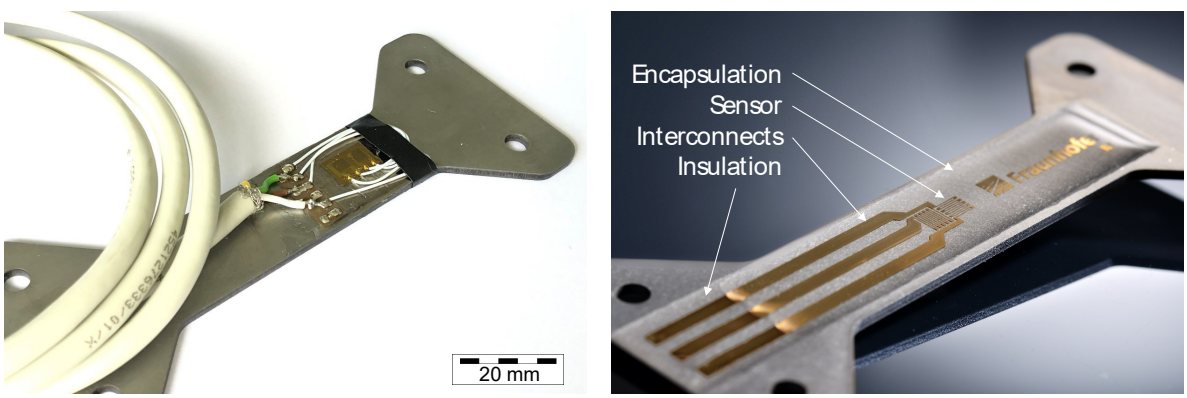

Fig. 5. Conventionally applied strain gauge (left) and additively manufactured strain gauge including interconnects (right)

For characterization, the accessible conductors (interconnects) are connected to a conventional measuring amplifier (HBM Quantum X MX440B) via spring contacts. The testing bar is fixed to a 3D printed plastic mount structure at both ends according to Figure 6.

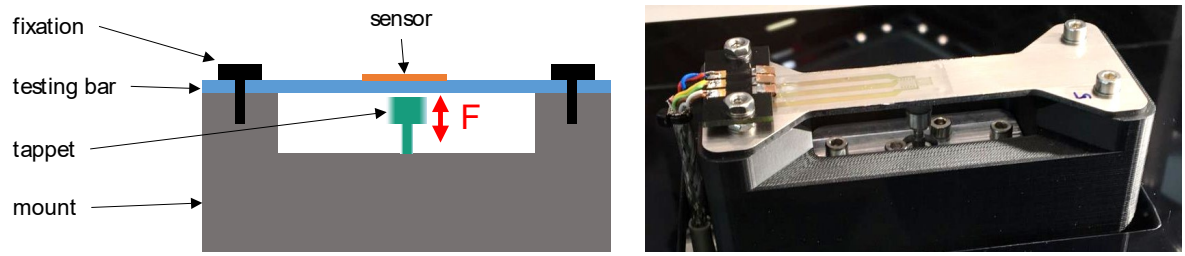

Fig. 6. Scheme of testing set-up (left), testing set-up (right)

A pneumatic driven tappet applies a periodic bending force that deforms the component and its connected strain sensor. Pressure is applied for 5.5 s while the release time is 11.5 s. The applied force is measured to 10 N, the displacement at the middle of the testing bar is measured to 5 µm. The measurement signal is depicted in Figure 7 and shows coincident change in the sensor signal to applied loads.

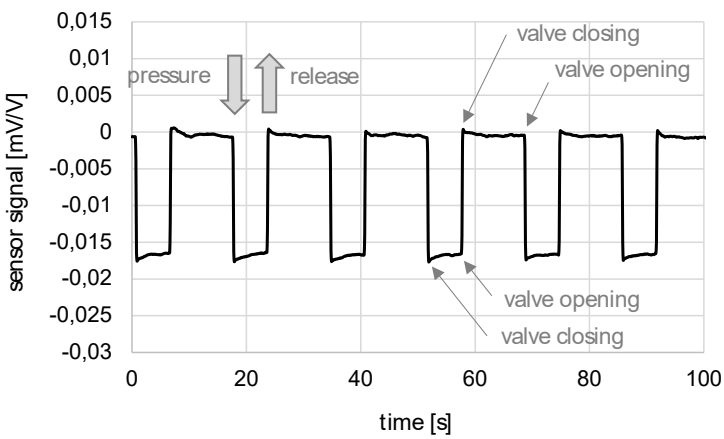

Fig. 7. Sensor response to application of force (measured data)

After applying pressure and closing the valve a recurring relaxation is observed which is most likely due to the poor rigidity of the plastic mount which was selected for demonstration purposes only. A thorough investigation of the sensor's performance is planned to be done in the near future.

4. Conclusion and Outlook

An advanced process chain for the additive manufacturing of component-connected strain gauges using print and laser technologies is presented and the process implementation demonstrated. Resistivities of conducting lines after laser sintering are compared to oven treated samples showing increased conductivities by a factor of about 2.2 in comparison the oven benchmark. The sensor function of an additively manufactured sensor on a metal testing bar is shown in a bending test scenario. The presented process chain aims at an approach for the economically feasible use of a new generation of additive sensors, focussing on auto-

mation, cost reduction in manufacturing and the consideration of industrial applicability with regards to robustness and metrological precision are in the future.

Besides all potential of the presented additive approach, there are still challenges to be faced, such as increasing reproducibility of printed layer thicknesses and structure geometries, transferring the printing and laser sintering processing of silver inks to constantan inks, implementing process control and quality management, transferring the process to apply sensors to complex 3D components, physically connecting the sensor to miniature (mobile) measuring equipment, collecting and transferring data etc., to name a few.
The benefit will be a fully automatable, digital in-line manufacturing process of embedded strain sensors and others, capable of making future production machines and products smarter.

References

[1] H. Kagermann, W.-D. Lukas, W. Wahlster, VDI-Nachrichten (1.April) 2.

[2] S. Keil, Dehnungsmessstreifen, 2nd ed., 2017.

[3] A. Krutsch, Untersuchung zu inkjetgedruckten Dehnungssensoren auf Foliensubstraten, 2015.

[4] O. Kravchuk, Y. Bobitski, M. Reichenberger, Laser curing of inkjet printed strain gauge structures, in: Proceedings of the 23rd International Conference Mixed Design of Integrated Circuits and Systems, MIXDES 2016: Łodź, Poland, June 23-25, 2016, Lodz, Poland, IEEE, Piscataway, NJ, 2016, pp. 343–345.

[5] M.J. Renn, M. Schrandt, J. Renn, J.Q. Feng, Localized Laser Sintering of Metal Nanoparticle Inks Printed with Aerosol Jet® Technology for Flexible Electronics, Journal of Microelectronics and Electronic Packaging 14 (2017) 132–139. https://doi.org/10.4071/imaps.521797.

[6] J. Keck, B. Freisinger, D. Juric, K. Glaser, M. Volker, W. Eberhardt, A. Zimmermann, Low-Temperature Sintering of Nanometal Inks on Polymer Substrates, in: 2018 13th International Congress Molded Interconnect Devices (MID): 25-26 Sept. 2018, Würzburg, IEEE, Piscataway, NJ, 2018, pp. 1–7.

[7] M. Elsobky, Y. Mahsereci, J. Keck, H. Richter, J.N. Burghartz, Design of a CMOS readout circuit on ultra-thin flexible silicon chip for printed strain gauges, Adv. Radio Sci. 15 (2017) 123–130. https://doi.org/10.5194/ars-15-123-2017.

[8] M. Maiwald, C. Werner, V. Zöllmer, M. Busse, INKtelligent printing ® for sensorial applications, Sensor Review 30 (2010) 19–23. https://doi.org/10.1108/02602281011010763.

[9] C. Vedder, S. Wollgarten, R. Gradmann, J. Stollenwerk, K. Wissenbach, M. Eberstein, Laser-based functionalization of electronic multi-material-layers for embedded sensors, Journal of Laser Applications 29 (2017) 22603. https://doi.org/10.2351/1.4983267.

[10] W. Zapka, Handbook of Industrial Inkjet Printing, Wiley-VCH Verlag GmbH & Co. KGaA, Weinheim, Germany, 2017.

[11] R. Eckstein, Aerosol Jet Printed Electronic Devices and Systems.

[12] J.-U. Park, M. Hardy, S.J. Kang, K. Barton, K. Adair, D.K. Mukhopadhyay, C.Y. Lee, M.S. Strano, A.G. Alleyne, J.G. Georgiadis, P.M. Ferreira, J.A. Rogers, High-resolution electrohydrodynamic jet printing, Nat. Mater. 6 (2007) 782–789. https://doi.org/10.1038/nmat1974.

[13] SIJTechnology Inc., Super Inkjet Printer. http://sijtechnology.com/en/products/.

[14] M. Birkett, R. Penlington, Laser Trimming of CuAlMo Thin-Film Resistors: Effect of Laser Processing Parameters, Journal of Elec Materi 41 (2012) 2169–2177. https://doi.org/10.1007/s11664-012-2103-9.

[15] Vishay Precision Group, Application Note - Using Laser Trimmable Resistors, 2013.

[16] R.D. Deegan, O. Bakajin, T.F. Dupont, G. Huber, S.R. Nagel, T.A. Witten, Capillary flow as the cause of ring stains from dried liquid drops, Nature 389 (1997) 827. https://doi.org/10.1038/39827.

Appendix A. UV/Vis spectra

The reflectance and transmittance spectra of printed silver and hybrid polymer layers were measured using a Lambda 1050 (Perkin Elmer) spectrometer (Figure 8 and Figure 9).

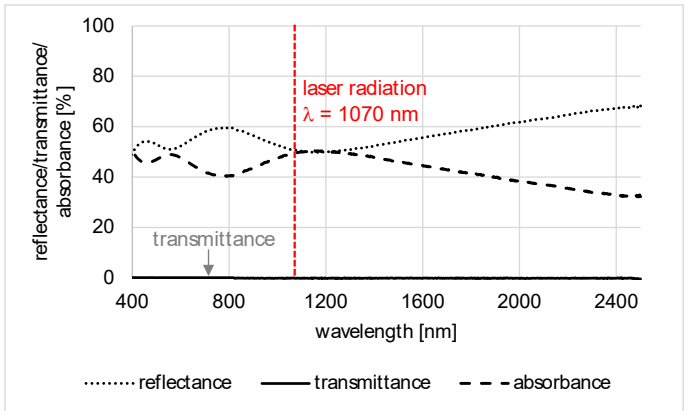

Fig. 8. UV/VIS/NIR spectra of an inkjet printed and dried silver layer (thickness approx. 1 µm)

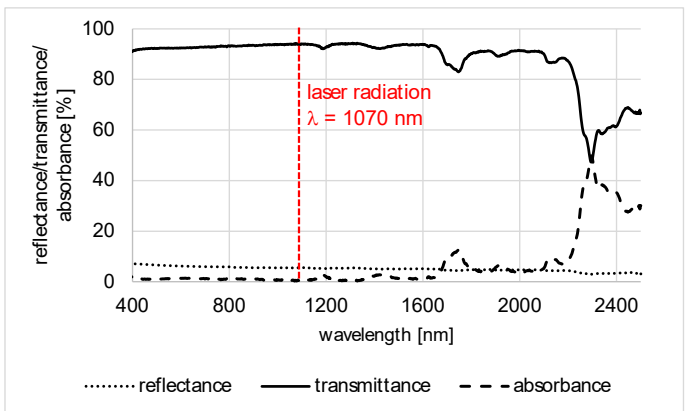

Fig. 9. UV/VIS/NIR spectra of a dispensed and UV-cured hybrid polymer layer (thickness approx. 220 µm)